Vol. 452: 45–61, 2012
doi: 10.3354/meps09704

MARINE ECOLOGY PROGRESS SERIES
Mar Ecol Prog Ser

Published April 25

Primary production throughout austral fall, during a time of decreasing daylength in the western Antarctic Peninsula

Maria Vernet[1,*], Wendy A. Kozlowski[1], Lynn R. Yarmey[1,4], Alexander T. Lowe[2,5], Robin M. Ross[2], Langdon B. Quetin[2], Christian H. Fritsen[3]

[1]Integrative Oceanography Division, Scripps Institution of Oceanography, La Jolla, California 92093-0218, USA
[2]Marine Science Institute, University of California, Santa Barbara, Santa Barbara, California 93106-6150, USA
[3]Division of Earth and Ecosystem Sciences, Desert Research Institute, Reno, Nevada 89512, USA

[4]*Present address:* National Snow and Ice Data Center, University of Colorado at Boulder, Boulder, Colorado 80309-0449, USA
[5]*Present address:* Friday Harbor Laboratories, University of Washington, Friday Harbor, Washington 98250, USA

ABSTRACT: Antarctic phytoplankton is characterized by a pronounced seasonality in abundance, driven mainly by changes in sunlight. We combined measurements and modeling to describe the influence of changing daylength on fall and winter phytoplankton production in coastal waters of the western Antarctic Peninsula (wAP) in 2001 and 2002. The model was parameterized with field observations from the Palmer Long-Term Ecological program in the wAP during summer and early fall and from the Southern Ocean Global Ecosystems Dynamics program fall and winter cruises to Marguerite Bay and shelf waters. Shorter daylength and a deepening of the mixed layer account for most of the decrease in primary production during March, April, and May. At this time, biomass decreases by an order of magnitude and remains low and constant until the end of August. An additional loss rate was added to the primary production model to fit output to observations. This loss rate, estimated at ~0.1 to 0.15 d^{-1}, is due to physical, chemical, and biological processes such as scavenging by sea ice, zooplankton grazing, cell lysis, and cell sedimentation, which are expected to be high at this time of year. Growth and loss rates of phytoplankton populations are similar on 1 March, with growth decreasing rapidly over time while the loss rates remain constant. By the beginning of winter (1 June), growth is low, with minimum rates in July and increasing towards September. During a period of diminishing food supply, preliminary estimates of grazing indicate that fall biomass could support existing macrozooplankton populations, but the timing and concentration of food supply is variable and expected to affect health of zooplankton as they enter the winter.

KEY WORDS: Phytoplankton · Primary production · Antarctica · Bloom demise · Fall · Winter · Growth rates · Loss rates

INTRODUCTION

The fall season is critical to phytoplankton dynamics in coastal Antarctic waters of the western Antarctic Peninsula (wAP). Shortening days and decreasing irradiance, increasing storminess, and ice formation combine to decrease the input and maximize the loss in phytoplankton accumulation (Pearce et al. 2008). Fall is a transition period between maximum insolation in December and January (18 to 24 h) and the short days or darkness characteristic of June and July (0 to 4 h). High phytoplankton biomass in the austral

*Email: mvernet@ucsd.edu

summer of 1 to 3 mg chlorophyll *a* (chl *a*) m^{-3} with peaks or blooms up to 30 mg m^{-3} (Smith et al. 1998) decreases to a low of <0.2 mg m^{-3} in the winter (Pakhomov et al. 2004, Fritsen et al. 2008, Meyer et al. 2009). In the fall, phytoplankton biomass is variable, with chl *a* concentrations anywhere from 0.1 to 2 mg m^{-3} within the surface mixed layer (Vernet et al. 2011).

Our knowledge of fall and winter phytoplankton dynamics in the Southern Ocean is limited by the difficulty of sampling underneath the ice and the lack of ocean color remote sensing images from April to October due to low sun angle (Marrari et al. 2008). This lack of information precludes understanding variability due to latitude and interannual changes in the water column. Scarce supply of food during winter (Smith et al. 1996) combined with low starvation tolerance of some zooplankton, e.g. larval krill, might necessitate their use of an alternative food source (Walsh et al. 2001). Several investigators (Daly 1990, Smetacek et al. 1990, Quetin & Ross 1991) have suggested that sea ice microbial communities (SIMCOs) might be an essential food resource for winter survival, and both behavioral and physiological evidence continues to support this concept (e.g. Marschall 1988, Stretch et al. 1988, Daly 1990, Quetin et al. 1996, Frazer et al. 1997, 2002, Meyer et al. 2002, 2003). The dependence of Antarctic krill larvae on phytoplankton population dynamics during austral fall is less known. Larval krill growth rates decrease rapidly during fall months until reaching a minimum in winter (Quetin et al. 2003). This evidence suggests that food may be limiting zooplankton growth during the fall and winter.

There is also a need to evaluate the importance of the incorporation of fall phytoplankton blooms into sea ice. Understanding this will allow estimates of sea ice-based primary production and subsequent winter larval krill physiological condition and survival. The assumption is that SIMCO biomass is a function of its growth within sea ice. However, there is increasing evidence that in the fall and winter the amount of cell scavenging from the water column into sea ice is critical (Fritsen et al. 2008). Scavenging by larval krill is a function of timing and extent of sea ice formation and of phytoplankton concentration at the time of frazil ice formation (Ackley et al.1982, Garrison et al. 1983, 1989).

Several important lines of inquiry with respect to the importance of phytoplankton dynamics and larval krill survival remain. These include understanding (1) phytoplankton availability (concentration and timing of decline) during fall months as primary production decreases due to shorter daylength and (2) phytoplankton availability in winter. With this understanding we can quantify phytoplankton and SIMCOs as a food source for larval krill through fall and winter, and (3) evaluate the relative importance of water column phytoplankton and SIMCOs as food sources for larval krill through fall, winter, and early spring. This paper addresses the first 2 topics, phytoplankton growth during austral fall and winter, and its role as potential food for zooplankton. Lowe et al. (2012, this volume) addressed the third topic, larval krill growth and condition factor based on phytoplankton and SIMCO concentrations (Fritsen et al. 2010).

We chose a modeling effort to describe daily phytoplankton concentrations and to evaluate the rate and interannual variability of bloom demise. The bio-optical model is parameterized with *in situ* data from representative locations along the central and south coastal areas of the wAP. Model results provide estimates of phytoplankton growth and loss terms through the fall and winter. We explore the effect of latitude and changing irradiance on the decline of the fall phytoplankton biomass, presented as chl *a*.

MATERIALS AND METHODS

Data on fall and winter phytoplankton biomass and primary production were collected in 2001 and 2002 from Palmer Basin near Palmer Station, Anvers Island (64.8° S, 64.6° W) and on the shelf off Marguerite Bay (68.0° S, 69.1° W) by 2 large interdisciplinary studies, the Palmer Long-Term Ecological Research (Pal LTER) and the Southern Ocean Global Ocean Ecosystems Dynamics (SO GLOBEC) projects (http://oceaninformatics.ucsd.edu/datazoo/data/pallter/datasets, http://globec.whoi.edu/jg/dir/globec/soglobec). These data allow the description of phytoplankton decline during 2 contrasting years, with low phytoplankton biomass and late ice formation for 2001 and the opposite for 2002. The data were used to parameterize the model of phytoplankton primary production and to simulate chl *a* concentrations during the fall and winters of 2001 and 2002.

Sampling

For Palmer Basin, modeling was done for a station (Stn B) within 3.2 km of Palmer Station (64.8° S, 64.6° W) in a water column depth of 96 m (Fig. 1). Samples for the estimation of phytoplankton biomass and primary production were obtained

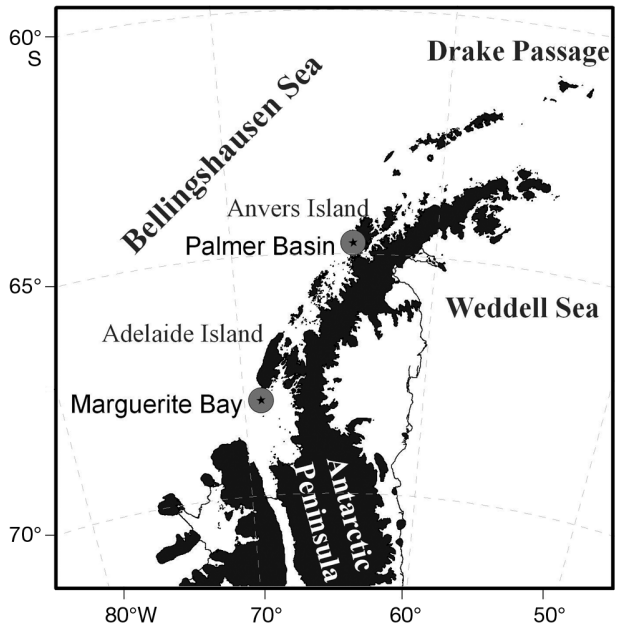

Fig. 1. Study sites in the western Antarctic Peninsula: Palmer Basin and mouth of Marguerite Bay (stars) at 64.8° S, 64.6° W and 68.01° S, 69.08° W, respectively

in 2001 and 2002 from a Mark V Zodiac during the growth season, October to March/April. Sampling frequency was twice weekly, Mondays and Thursdays, unless weather conditions prevented boating operations. In such cases, sampling was conducted on the first day that boating operations began again. After mid-April, sampling for phytoplankton biomass was done only from the station's seawater intake, located in Arthur Harbor, about 10 m away from shore and at an average depth of 5 m. Modeling in Marguerite Bay was done for a station at 68.0° S, 69.1° W in a water column depth of 260 m, corresponding to station 335.060 in the SO GLOBEC grid (Hofmann et al. 2004) and 208.-044 in the Pal LTER grid (Waters & Smith 1992). Phytoplankton biomass and production were determined during fall and winter cruises on board the RVIB 'Nathaniel B. Palmer' (NBP) in 2001 (23 April to 6 June, 21 July to 6 September) and 2002 (9 April to 21 May, 31 July to 17 September). Samples for biomass and primary production were collected from Go-Flow 5 l bottles in Palmer Basin or from 10 l Niskin bottles attached to the conductivity-temperature-depth (CTD) rosette on the ship, as well as from a bucket when necessary. In Palmer Basin, water was sampled at the surface and from depths corresponding to 50, 25, 10, 5, and 1% of incident irradiance, whereas during the SO GLOBEC cruises, water was sampled at fixed depths, viz. surface, 5, 10, 15, 20, 30, and 50 m.

Determination of chlorophyll and primary production

Chl *a* was determined with a Turner Designs Digital 10-AU-005-CE fluorometer (serial number 5333-FRXX), calibrated using a chl *a* standard from Sigma Chemical dissolved in 90% acetone (Holm-Hansen et al. 1965), and quantified with a spectrophotometer (Jeffrey & Humphrey 1975).

Chl *a* levels at the mouth of Marguerite Bay on 1 March 2001 and 2002 were estimated from Level 2 data from remote sensing SeaWiFS (Sea-viewing Wide Field-of-view Sensor). Although variability between SeaWiFs and *in situ* estimates are expected, several studies have shown a positive correlation between field-measured and remotely sensed chl *a* concentrations for the wAP (e.g. Dierssen & Smith 2000).

Estimates of primary production (PP) in Palmer Basin were made experimentally at each station with samples taken simultaneously with chl *a* determinations. On the NBP, PP experiments were done approximately once per day, with an attempt to sample evenly both in- and offshore, and in the northern and southern parts of the SO GLOBEC grid and within Marguerite Bay. PP was estimated during 24 h on-deck incubations in UV opaque plexiglass incubators placed in a shade-free area on deck (simulated *in situ* experiments), with temperature maintained at surface *in situ* conditions with running sea water (range from −2 to +3°C). Duplicate 100 ml samples were incubated in 125 ml borosilicate bottles after addition of 1 µCi of $NaH^{14}CO_3$ per bottle. After 24 h, the samples were concentrated onto 25 mm Whatman GF/F filters, fumed with 20% HCl for 24 h and placed in 5 ml of Universol scintillation fluid. Samples were then counted on a scintillation counter (Wallac 1409). Specific activity of each sample depth was determined from 0.1 ml of sea water after ^{14}C inoculation. Time-0 values, determined from filtration of a 100 ml sample before incubation, were always <5% of the light data (data not shown). PP was calculated from the difference between light and dark bottle readings and assuming an HCO_3^- in the water of 24 g C kg^{-1} (Carrillo & Karl 1999). Photosynthetic parameters were calculated from these PP versus irradiance relationships with the formulations of Platt & Jassby (1976) and Platt et al. (1980).

Surface and underwater irradiance and daylength

For Palmer Basin, daily integrated surface photosynthetically available radiation (PAR) was calculated either from the Biospherical Instruments (BSI) Profiling Reflectance Radiometer (PRR) reference sensor estimating surface irradiance (E_s) or from the BSI Ground UV (GUV) sensor located in Palmer Basin, with units of µE m^{-2} d^{-1}. On the ship, light data were collected with a BSI GUV radiometer, mounted on the science mast, configured with a PAR channel, and with channels for 305, 320, 340, and 380 nm wavelengths. Additional PAR data were collected with a BSI QSR-240 sensor, also mounted on the science mast. Recording of both surface and profiling PAR was conducted throughout the sampling duration of the cruises. GUV data were collected at 1 min intervals and logged directly to a computer. QSR data were collected 2 ways: (1) as part of the meteorological data set, logged as raw voltage; and (2) onto a LICOR LI-1000 data logger, also logged as raw voltage, but with 4 additional decimal points for increased resolution. A comparison of the 2 instruments was done to determine collection differences between the 2 types (scalar versus cosine) of sensors (data not shown).

A BSI PRR-600 on free-fall mode from the Mark V Zodiac, deployed in a shade-free area, was used to measure the underwater irradiance profile and also to determine sampling depths based on light levels. On board the NBP, PAR data were collected during each CTD cast using a profiling PAR sensor, the BSI QSL-250.

Daylength was calculated as per Forsythe et al. (1995) with input for latitude and year day (YD). The values were compared to the US Naval Office tables to check for accuracy (http://aa.usno.navy. mil/).

Euphotic zone depth (Z_{eu}) and mixed layer depth (MLD)

Z_{eu} was defined as the depth of 1% surface irradiance, and is the surface layer where net PP occurs (carbon uptake > respiration). Z_{eu} was calculated as:

$$Z_{eu}\,(\mathrm{m}) = \ln[\mathrm{PAR}\,(1\%) / \mathrm{PAR}\,(0\ \mathrm{m})] / -\mathrm{Kd}_{\mathrm{PAR}} \quad (1)$$

where PAR is in µE m^{-2} s^{-1} and Kd_{PAR} (m^{-1}) is the diffuse attenuation coefficient at that station.

The seasonal development (i.e. deepening) of the MLD was estimated from 1993 summer (January), fall (April and May), and winter (August) cruises to the wAP. MLD was calculated as the local maxima of the second derivative of the downcast density profile (Martinson & Iannuzzi 1998). Inshore stations, within 30 km of the coast, were not sampled in the winter due to heavy ice.

Modeling primary production: fall and winter phytoplankton

Seasonal concentrations of chl *a* for fall (March, April, and May, MAM) and winter (June, July, and August, JJA) were estimated from modeled PP and a seasonally varying carbon:chlorophyll (C:chl *a*) ratio (Table 1; Garibotti et al. 2003). Integrated PP estimates of carbon increase were based on daily increments within the euphotic zone. The empirical bio-optical model was developed by Dierssen et al. (2000) with field data from the wAP following formulations by Behrenfeld & Falkowski (1997):

$$\mathrm{PP}_i(z) = P^{\mathrm{B}}{}_{\mathrm{opt}} \times \mathrm{DL}i \times \mathrm{Chl}a_i \times z_i \times F \quad (2)$$

where $PP_i(z)$ is the integrated PP (mg C m^{-2} d^{-1}) for day *i*, $P^{B}{}_{opt}$ is the chl *a*-normalized maximum rate of underwater photosynthesis (mg C [mg chl *a*]$^{-1}$ h^{-1}), DL is photoperiod estimated by daylength (h), Chla_i is the average chl *a* concentration (mg m^{-3}) for day *i*, *z* is the depth of integration within the euphotic zone (in m) or MLD (in m) for day *i*, whichever is shallower, and *F* is the empirically estimated ratio of mean chl *a*-normalized productivity in the water column to $P^{B}{}_{opt}$, calculated as:

$$F = E_{\mathrm{d}}(0^+) / [E_{\mathrm{d}}(0^+) + 11.77] \quad (3)$$

where $E_d(0^+)$ is daily downwelling irradiance (400 to 700 nm) incident upon the sea surface (µE m^{-2} d^{-1}). In this model, each component is individually regressed against PP_i (z) (Dierssen et al. 2000). *F* values were tested by comparing results of the model to *in situ* measurements of PP.

Biomass within the euphotic zone was calculated by adding daily increments of biomass, i.e. converting daily integrated PP from C to chl *a*, and adding it to the chl *a* of the previous day:

$$\mathrm{Chl}a_i\,(z) = (\mathrm{Chl}a_{i-1}(z) + \mathrm{PP}_i(z) \times \mathrm{Chl}a{:}\mathrm{C}) \times \mathrm{LF} \quad (4)$$

where chla_i and chla_{i-1} are the water column integrated chl *a* of the day and the previous day in mg m^{-2}, PP_i (z) is the daily PP from Eq. (2), Chl*a*:C is the chl *a* to phytoplankton carbon ratio, and LF is an empirical loss factor to account for any additional

Table 1. Parameters used in modeling phytoplankton primary production at Palmer Basin (Pal Bas; 64° S) and the mouth of Marguerite Bay (M Bay; 68° S) in fall (March, April, May) and winter (June, July, August) of 2001 and 2002. P^B_{opt}: average is calculated from the stations where photosynthesis saturation with light was encountered. Others not included did not reach saturation. Same P^B_{opt} used for fall and winter as in winter saturation was almost never reached. LF: empirical loss factor to adjust model to observations, where LF < 100. YD: year day; PAR: photosynthetically available radiation (µmol photons m^{-2} d^{-1}); chl *a*: chlorophyll *a* (mg m^{-2}); na: not applicable

Variable	Definition	Obervation site/period	Fall	Winter	Units
chl_o	1 March phytoplankton concentration	Pal Bas '01 Pal Bas '02 M Bay '01 M Bay '02	2.6 5.3 0.5 2.7	na na na na	mg m^{-3}
P^B_{opt}	Maximum photosynthetic rate	Pal Bas '01 Pal Bas '02 M Bay '01 M Bay '02	1.22 ± 0.34 1.33 ± 0.43 1.12 ± 0.14 0.92 ± 0.37	1.22 ± 0.34 1.33 ± 0.43 1.12 ± 0.14 0.92 ± 0.37	mg C (mg chl *a*)$^{-1}$ h^{-1}
DL	Daylength	Pal Bas M Bay	14.48 to 4.52 14.88 to 2.01	3.52 to 9.71 0 to 9.28	h
F	Efficiency of photosynthesis		0.39	0.39	Dimensionless
Z_{eu}	Euphotic zone depth		ln [PAR (1%) / PAR (0 m)] × $(-Kd_{PAR})^{-1}$		m
Kd_{PAR}	Diffuse attenuation coefficient	2001 2002	0.0739 × ln (chl *a* + 1) + 0.0539 0.1082 × ln (chl *a* + 1) + 0.0559		m^{-1}
C:chl *a*	Carbon-to-chl *a* ratio	–	75	50	Dimensionless
MLD	Mixed layer depth	–	−13.99 + 0.6229 × YD		m
LF	Loss factor (fraction of biomass lost per day)	Pal Bas '01 Pal Bas '02 M Bay '01 M Bay '02	9 9–15 6.5 7	9 15 6.5 7	%

decrease in biomass, expressed as a fraction of the chl *a* ($chla_i$) concentration (LF < 100) and expressed in the text as a percentage (%). LF was needed to fit the daily production to observed data. The resulting biomass represented the net daily change in chl *a* concentration ($chla_{inet}$). In comparison, gross chl *a* ($chla_{ig}$) is based on the change in daily chl *a* due to PP (Eq. 2).

Specific growth rate (µ, d^{-1}) was calculated from the daily gross $chla_{ig}$ increments per day *i* (d) based on Eq. (2) as:

$$\mu_i = \ln (chla_{ig} / chla_{ig-1}) \times d^{-1} \quad (5)$$

The daily loss rate (LR) can also be expressed in d^{-1} as the difference between the specific growth rate (Eq. 5) and daily net $chla_{inet}$ changes based on Eq. (4) as:

$$LR_i (z) = \mu_i - [\ln (chla_{inet-1} / chla_{inet}) \times d^{-1}] \quad (6)$$

Combining Eqs. (5) and (6), net community growth can be calculated as $\mu_i - LR_i$.

Statistics

The data were often not normally distributed. Differences between seasons and years were assessed with the non-parametric Kruskal-Wallis test (Zar 1999), which is based on the ranks of the data rather than the values. Data are presented as mean ± SD. Significance is given for $\alpha = 0.05$ and $\alpha = 0.01$.

As a measure of the predictive power of the model, the root mean square error (RMSE; Ott & Longnecker 2001) was calculated for the Palmer Basin 2001 and 2002 models. RMSE was then normalized to the range of measured values and thus expressed as a percentage of chl *a*.

RESULTS

Environmental parameters

Seasonal data collected from near Palmer Station, Anvers Island, were used to parameterize the model

for Palmer Basin. These numbers are mostly for the growth season, from October to April, with the exception of the seawater intake biomass collected year round. Similarly, biomass and PP measurements from the fall and winter cruises to Marguerite Bay and adjacent shelf waters provided biomass and PP for the modeling for Marguerite Bay. Ocean color images supplemented the biomass estimates for this area in late summer (1 March) before ship-board samples were taken.

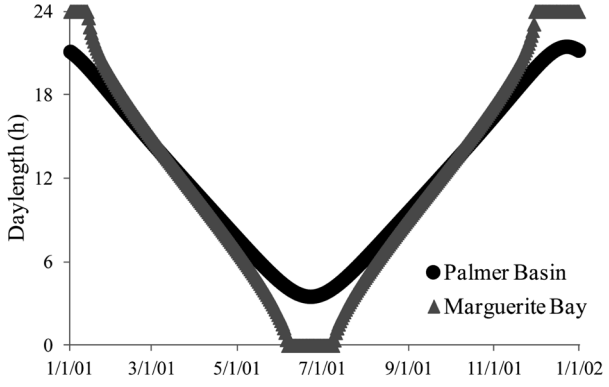

Fig. 2. Daylength (h) at Palmer Basin (Stn B in Arthur Harbor, black) and mouth of Marguerite Bay (SO GLOBEC station 208.-044, grey) where the model was developed. Dates on *x*-axis are shown as m/d/yy

Surface irradiance

Irradiance at high latitude is influenced by sun angles (sun height over the horizon). This factor is included in the model as integrated daily irradiance or daylength, in hours of light. The main difference between the 2 sites in this study is in summer and winter, where at higher latitudes (i.e. Marguerite Bay, Fig. 2) winters reach total darkness for ~4 wk and summers are longer (~4 wk of 24 h sunlight). The Palmer Basin region has a minimum of ~4.4 h sunlight in the winter and a maximum of ~19.7 h sunlight in the summer.

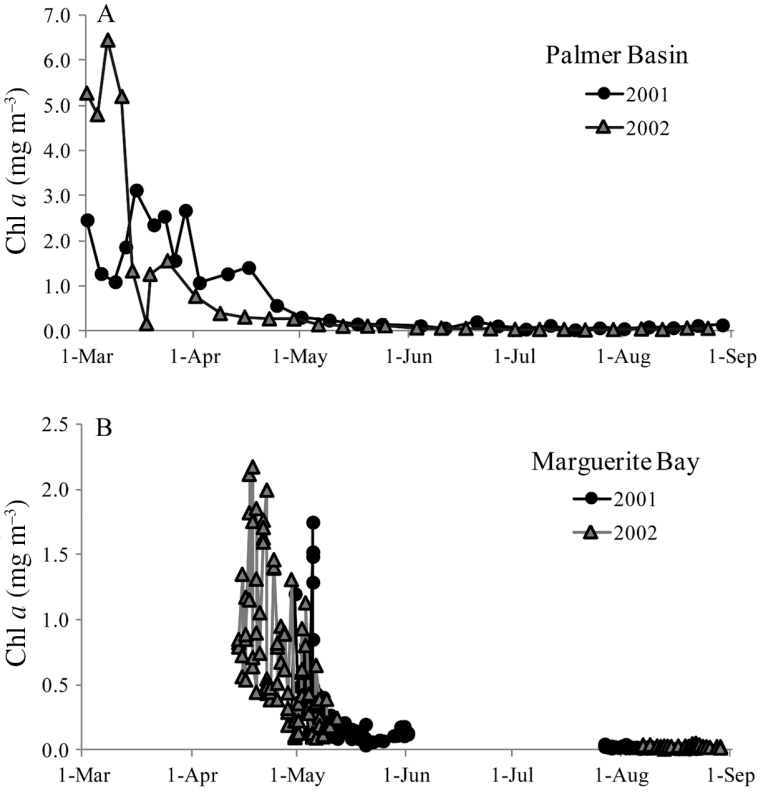

Fig. 3. Phytoplankton biomass as chlorophyll *a* (chl *a*; in mg m^{-3}) at (A) Palmer Basin, from 3 to 5 m, measured from bi-weekly samples as taken from the seawater intake in 2001 and 2002 and (B) Southern Ocean GLOBEC cruises in fall and winter of 2001 and 2002 sampled at 5 m depth. Note differences in scale between panels

Fall and winter phytoplankton biomass

Measured chl *a* concentration in late summer started high (~2 mg m^{-3}), decreasing by a factor >10 from March to June and remaining low throughout the winter. For Palmer Basin, average chl *a* concentration was 1.55 ± 1.68 mg m^{-3} in fall (MAM) and 0.077 ± 0.044 mg m^{-3} in winter (JJA; Fig. 3A). For the Marguerite Bay area, chl *a* concentration was 0.50 ± 0.49 mg m^{-3} and 0.031 + 0.026 mg m^{-3} in fall and winter, respectively (Fig. 3B).

There was measurable interannual variability, most noticeable at the beginning of fall. Average concentration in March in Palmer Basin was 1.5 times higher in 2002 than in 2001 (3.25 versus 2.11 mg m^{-3}, respectively; Fig. 3A). This variability was not observed for the entire fall season, however, resulting in no significant difference in average chl *a* concentrations between 2001 (1.43 ± 0.96 mg m^{-3}) and 2002 (1.68 ± 2.21 mg m^{-3}; Kruskal-Wallis, $p = 0.293$). Significant differences were observed in winter chl *a*, with average concentrations of 0.104 ± 0.048 mg m^{-3} in 2001 and 0.050 ± 0.015 mg m^{-3} in 2002 (Kruskal-Wallis, $p < 0.01$).

Interannual variability in the Marguerite Bay area in chl *a* concentration from remote sensing data was observed on 1 March (0.34 ± 0.078 mg m^{-3}, n = 3, and 2.55 ± 1.92 mg m^{-3}, n = 6, in 2001 and 2002, respectively). Average concentrations in this area were twice as high in 2002 than in 2001 (0.69 ± 0.53 mg m^{-3} versus 0.29 ± 0.33 mg m^{-3} in the fall, Kruskal-Wallis, $p < 0.01$, and 0.040 ± 0.029 mg m^{-3} versus 0.023 ± 0.019 mg m^{-3} in the winter, Kruskal-Wallis, $p < 0.01$; Fig. 3B).

Diffuse attenuation coefficient

Differences in phytoplankton biomass are correlated with changes in water transparency. Therefore, Kd_{PAR} (m^{-1}) was determined from chl *a* concentration (transformed as $t(x) = \ln(x+1)$) and light distribution measured by the PRR-600 in 2001 and 2002 (Fig. 4). The values obtained for the wAP are similar to Stambler et al. (1997) for the Admundsen and Bellingshausen Seas and to Figueroa (2002) in the Gerlache Strait but lower than Mitchell & Holm-Hansen (1991b) in the Bransfield Strait.

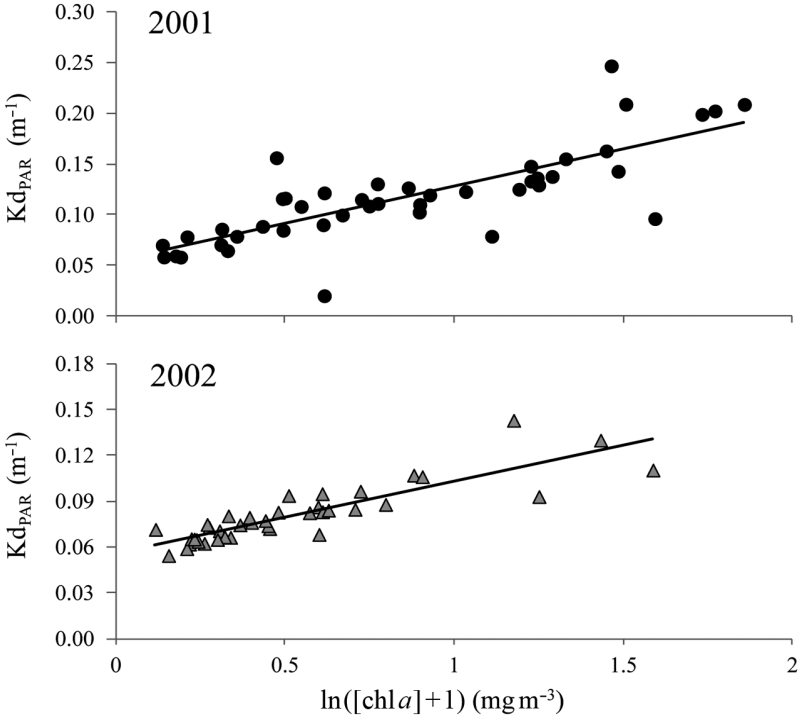

Fig. 4. Relationship between the diffuse attenuation coefficient for photosynthetically available radiation (Kd_{PAR}) and chlorophyll *a* ([chl *a*]) concentration for January 2001 and January 2002, between 64° S and 68° S on the shelf west of the Antarctic Peninsula. For 2001, $Kd_{PAR} = 0.028$ chl *a* + 0.0707, $r^2 = 0.75$, and for 2002, $Kd_{PAR} = 0.0201$ chl *a* + 0.0656, $r^2 = 0.89$

Photosynthetic parameters

The determination of P^B_{opt} or maximum photosynthetic rate in the water column is a key parameter in the model. The depth of P^B_{opt} varied from ~15 to ~2 m, corresponding to 12.5 to 50% incident PAR, which ranged from a daily average of 300 to 75 µE m^{-2} s^{-1} in Palmer Basin (Fig. 5A). Late fall irradiance in the Marguerite Bay area was 10 times lower than in Palmer Basin, from a daily average of 75 to 5 µE m^{-2} s^{-1}. By late April, PP was light limited, reaching saturating photosynthesis only on some days (Fig. 5B). To calculate P^B_{opt}, we averaged the maximum production rate at the stations with saturating irradiance for each location and year (Table 1, Fig. 5).

Mixed layer depth

The deepening of the mixed layer with time in coastal areas is represented by the equation MLD (m) = −13.99 + 0.6229 × YD. Average MLDs for the entire region for summer are less than half those in fall and winter (Table 2).

Efficiency factor based on light, *F* calculation for the fall

Dierssen et al. (2000) provided an average *F* value of 0.64 for the wAP in the summer. This average was found to adequately represent *F* for modeling daily PP despite high short-term variability of up to a factor of 4×. To test its validity later in the season, *F* was calculated from the March data in Palmer Basin during 2001 and 2002 (n = 28), based on the E_s calculation from light attenuation or the $E_d(0^+)$ surface measured with the PRR-600. An $F = 0.388 \pm 0.127$ was obtained from E_s, with $E_d(0^+)$ giving comparable results, all similar to Stambler et al. (1997).

Model results: chlorophyll decline

The model was run from 1 March to 1 September of each year. The model calculates daily integrated PP within the Z_{eu} between surface and either the depth at 1% surface PAR or the MLD,

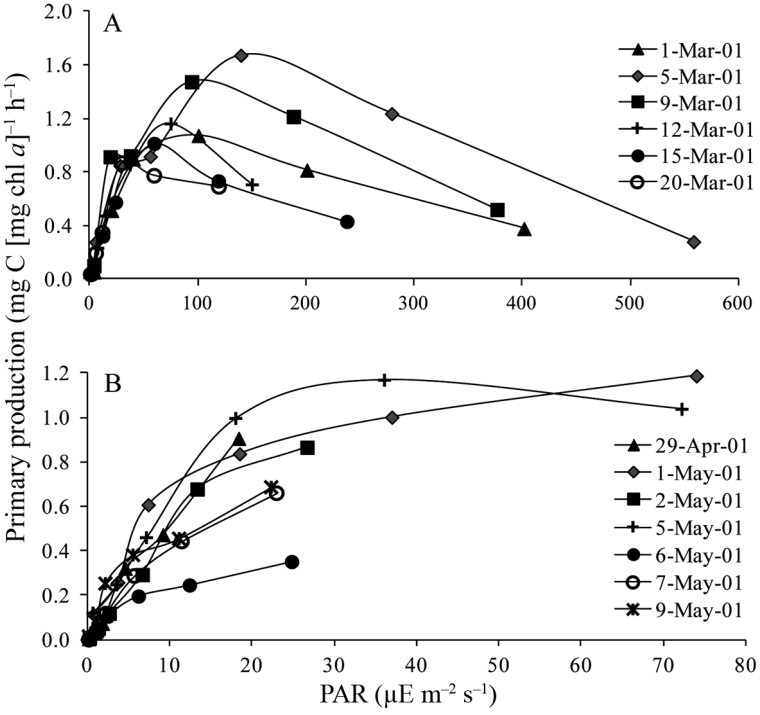

Fig. 5. Primary production as a function of the average daily photosynthetically available radiation (PAR). Data obtained from estimates of daily carbon incorporation in simulated *in situ* experiments and corrected for daylength and biomass. (A) Palmer Basin 2001; (B) Marguerite Bay 2001

Table 2. Mean (± SD) mixed layer depth (MLD) in Antarctic coastal waters estimated from seasonal cruises to the area. YD: year day

	Start (YD)	End (YD)	MLD (m)
Summer 1993	7	37	21.9 ± 22.6
Fall 1993	87	128	64.4 ± 23.8
Winter 1993	241	264	93.2 ± 28.4
Summer 1994	11	38	28.6 ± 19.5

whichever is shallower. Initial chl *a* values in the water column to start the model on 1 March were taken from all available field data and from the SeaWiFS satellite for the mouth of Marguerite Bay (68° S; Table 1). The fall to winter transition was assumed to be on 1 June, with changes in C:chl *a* ratio from 75 (Mitchell & Holm-Hansen 1991a, Garibotti et al. 2003) to 50, to account for cells richer in pigment due to low-light adaptation, and changes in P^B_{opt} (Table 1). Model results were compared to measured values from Palmer Basin and those measured *in situ* during the SO GLOBEC fall and winter cruises starting 1 May 2001 and 15 April 2002. LF (% daily decrease in biomass, Table 1) was introduced to bring modeled values in line with observed values.

Chl *a* decline in the fall in Palmer Basin was modeled for 2001 and 2002 with values, respectively, for P^B_{opt} of 1.22 and 1.33 mg C (mg chl *a*)$^{-1}$ h^{-1}, *F* of 0.39 for both years, initial chl *a* as measured on 1 March of 2.6 mg m^{-3} and 5.3 mg m^{-3}, and estimated LFs of 9 and 15% (Table 1, Fig. 6). In 2002, LF increased from 9 to 15% before April. The decline in chl *a* occurred in about 3 mo, reaching winter values by 1 June (Fig. 6, open triangles). The bloom demise was slower in 2001, showing 35% of the 1 March biomass by 15 April (Fig. 6A). In contrast, loss of biomass in 2002 was faster, with biomass reaching close to winter values by the end of April (Fig. 6B). Chl *a* concentrations after 1 June and during the winter are monotonic; modeled concentrations were <0.05 mg m^{-2} and representative of observed values (Fig. 6). In Marguerite Bay, the initial chl *a* values used for 2001 and 2002, respectively, were 0.5 and 2.7 mg m^{-3} (Fig. 7), i.e. higher in 2002, and were 6.5 and 7% for LFs (Table 1). Similar to Palmer Basin, winter values were reached by the beginning of June. However, biomass at significantly greater than winter concentrations extended later in the season in Marguerite Bay than in Palmer Basin. The model was better constrained for Palmer Basin than for Marguerite Bay due to the paucity of field data in the south. However, the higher 2002 biomass documented from the SO GLOBEC cruises (Fig. 3B) was well represented by the 1 March remote sensing values and allowed the model to estimate higher PP (Fig. 7B).

Chl *a* decline occurs as daylength decreases from 14.5 to 4.5 h in Palmer Basin (Fig. 2), decreasing PP by 2 orders of magnitude from highs of 427 and 953 mg C m^{-2} d^{-1} at the beginning of March in 2001 and 2002, respectively, to between 0.0003 and 4.405 mg C m^{-2} d^{-1} (Table 3). Growth rates during this period were low (range: 0.026 to 0.087 d^{-1}) with a minimum in mid-June (data not shown). Estimated loss rates remained constant through the fall and winter, but were higher in 2002 (range: 0.087 and 0.157 d^{-1}, in 2001 and 2002, respectively). In general, growth and loss rates were of similar magnitude on 1 March and diverged as the season progressed (Table 3). In Marguerite Bay, chl *a* decline occurs as daylength decreases from 14.9 to 2.0 h (Fig. 2), also decreasing PP by 2 orders of magnitude from highs of 75 and 345 mg C m^{-2} d^{-1} at the beginning of

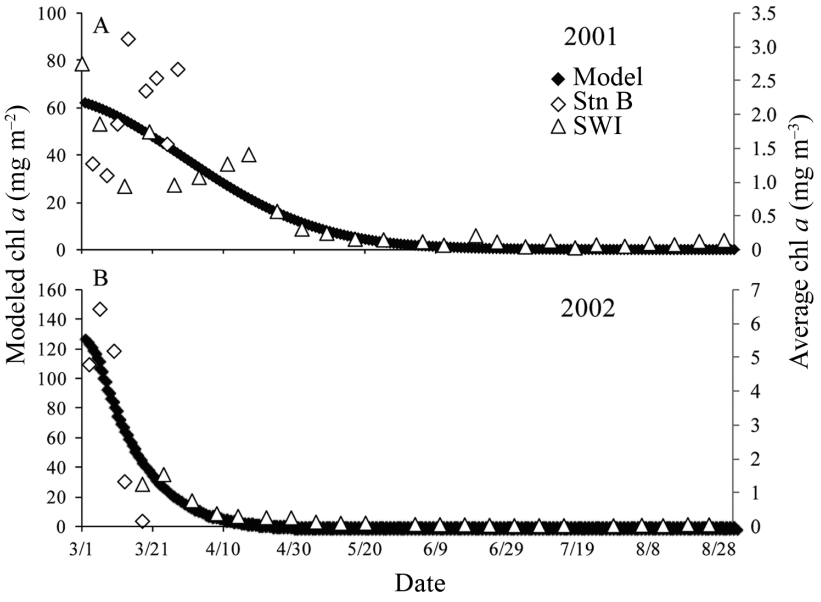

Fig. 6. Chlorophyll *a* (chl *a*) decline in Palmer Basin from model output compared to input biomass for (A) 2001 and (B) 2002. Note differences in scale between panels and with respect to Fig. 7. Measured chl *a* from Stn B (◇) and from the seawater intake (SWI; △) is average chl *a* in the euphotic zone (right axis, mg m^{-3}), whereas modeled output (◆) is integrated chl *a* within the euphotic zone (left axis, mg m^{-2}). The scales on both axes are approximately proportional to each other. Dates on *x*-axis are shown as m/d

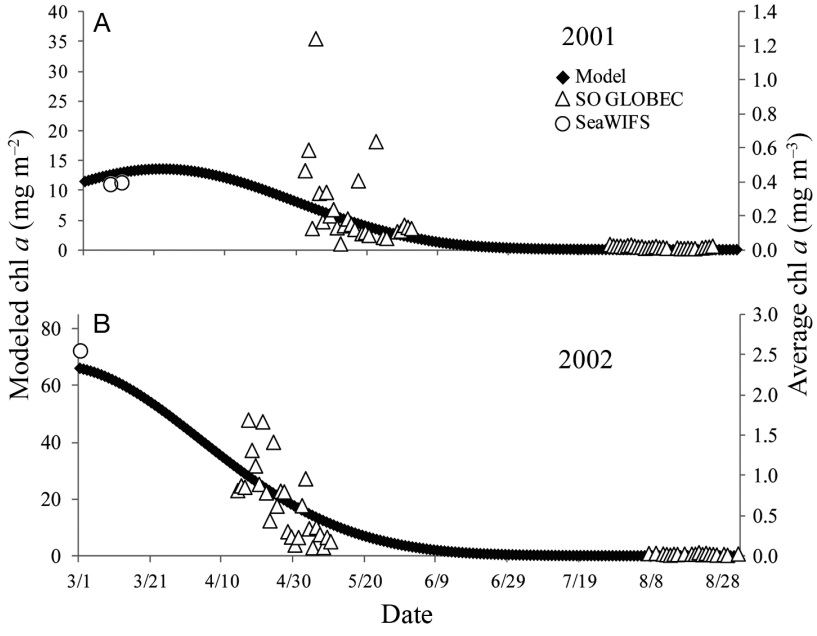

Fig. 7. Chlorophyll *a* (chl *a*) decline in Marguerite Bay from model output, compared to *in situ* chl *a* for (A) 2001 and (B) 2002. Note differences in scale between panels and with respect to Fig. 6. Measured chl *a* from cruises (△) and remote sensing (○) is average chl *a* in the euphotic zone (right axis, mg m^{-3}), and modeled output (◆) is integrated chl *a* within the euphotic zone (left axis, mg m^{-2}). The scales on both axes are approximately proportional to each other. Dates on *x*-axis are shown as m/d

March in 2001 and 2002, respectively (Table 3). Growth rates were low in the fall (range: 0.009 to 0.077 d^{-1}) and lowest in winter (range: 0.000 to 0.073 d^{-1}). PP and growth rates were 0 in Marguerite Bay between 6 June and 8 July, during darkness. Similar to Palmer Basin, loss rates remained constant through the fall and winter, at 0.062 to 0.073 d^{-1}. An initial recovery in water column production was observed at the end of August. At this time, MLD was ~138 m while the Z_{eu} was estimated at ~85 m (Table 3). As a result, biomass remained low during late winter (Table 3) while daily growth rates increased after a mid-winter minimum (data not shown).

Sensitivity analysis

Phytoplankton dynamics were sensitive to changes in the rate of phytoplankton decline (LF) and the C:chl *a* ratio of suspended biomass. A 5% increase in LF resulted in chl *a* reaching winter values in May, whereas a 5% decrease in LF was not able to control biomass increase due to phytoplankton growth in the fall, and chl *a* remained high (~2 mg m^{-3}) throughout the winter. A 5% decrease in the C:chl *a*, or algae richer in chl *a* as might be expected under lower irradiance conditions, produced a 20% increase in the fall biomass and 30% increase in winter. A 5% increase in the C:chl *a* resulted in a 40% lower biomass throughout fall and winter. The model was also sensitive to parameters for estimating PP. A 10% increase in either P^{B}_{opt} or *F* produced 50% more biomass and a 10% decrease in either of these parameters decreased biomass by 50% by mid-May and by 100% by the end of winter. With the exception of decreasing LF, changes in the variables did not alter the general behavior of the model but affected overall biomass and the timing of events, particularly the beginning of winter conditions.

Table 3. Output from the model, with phytoplankton (growth, primary production and chlorophyll *a* [chl *a*] concentration), optical (mixed layer and euphotic zone) and loss rates. Values are expressed as a mean or a range, from fall into winter (March, April, May), and winter (June, July, August). The calculated loss rate (LR) is based on the net daily change in chl *a*; μ is growth rate based on production rates, PP is integrated daily primary production, chl *a* is biomass as chl *a*, Z_{eu} is the depth of the euphotic zone defined as depth of 1% surface photosynthetically available radiation (PAR), and MLD is mixed layer depth. Significant differences between years were calculated using the Kruskal-Wallis test and are shown using asterisks in the 2001 median data fields for the PP, chl *a*, μ, and LR variables, where *α = 0.05, **α = 0.01

	PP (mgC m^{-2} d^{-1})	Chl *a* (mg m^{-3})	μ (d^{-1})	LR (d^{-1})	Z_{eu} (m)	MLD (m)
Palmer Basin						
2001 Fall						
Min.	4.73	0.027	0.026	0.087	48.1	24.0
Max.	427.4	2.304	0.080	0.092	84.1	80.7
Median	102.3**	0.443**	0.052**	0.089**	70.0	52.3
2001 Winter						
Min.	0.193	0.001	0.030	0.087	84.2	81.3
Max.	4.405	0.026	0.080	0.091	85.4	138.0
Median	0.355**	0.002**	0.042	0.090**	85.4	109.7
2002 Fall						
Min.	0.074	0.000	0.039	0.097	33.0	24.0
Max.	953.6	5.329	0.087	0.156	82.4	80.7
Median	16.23	0.065	0.060	0.153	79.6	52.3
2002 Winter						
Min.	0.000	0.000	0.031	0.149	82.4	81.3
Max.	0.065	0.0003	0.082	0.157	82.4	138.0
Median	0.0003	0.0000	0.042	0.155	82.4	109.7
Marguerite Bay						
2001 Fall						
Min.	1.749	0.028	0.011	0.062	69.0	24.0
Max.	75.92	0.479	0.077	0.067	84.1	80.7
Median	42.45**	0.212**	0.047**	0.064**	76.6	52.3
2001 Winter						
Min.	0.000	0.001	0.000	0.062	84.1	81.3
Max.	1.435	0.026	0.073	0.067	85.4	138.0
Median	0.146**	0.001*	0.022	0.066**	85.4	109.7
2002 Fall						
Min.	2.320	0.046	0.009	0.068	38.7	24.0
Max.	349.3	2.750	0.064	0.072	79.4	80.7
Median	92.83	0.565	0.038	0.070	59.7	52.3
2002 Winter						
Min.	0.000	0.000		0.068	79.6	81.3
Max.	1.887	0.043		0.073	82.3	138.0
Median	0.119	0.002		0.071	82.2	109.7

DISCUSSION

Fall and winter phytoplankton patterns

The simple light-driven model used in this study accurately reproduced changes in phytoplankton biomass between March and September at 2 coastal sites on the wAP, and the transition from summer maximum (January) to winter minimum (July), and provides estimates for periods without field data (Figs. 6 & 7). Low biomass based on reduced production was observed throughout the 3 winter months (JJA). To place our model results in the context of the seasonal development, we show integrated PP for the years 2001 and 2002 in Palmer Basin (Fig. 8). The low phytoplankton biomass extends beyond winter, with chl *a* accumulation in the water column delayed to early October. This agrees with our model of low production in the water column at the end of August (i.e. production is ~70% dependent on biomass, Dierssen et al. 2000). Thus, onset of production in the water column in the winter to spring transition lags by 1 to 2 mo behind the increase in daylength. Two factors could maintain winter conditions in September in the water column: the presence of sea ice and/or a deep mixed layer. Sea ice will limit penetration of surface irradiance in the water column at a time of increasing daylength, restricting growth. The MLD is estimated to be 138 m by the end of August (Table 3) and is not expected to shoal until sea ice melts (Vernet et al. 2008). In contrast, growth can be observed in SIMCOs during August, as soon as daylength increases, and remains high until sea ice melts (Lowe et al. 2012). The interaction between water column PP and sea ice results in an asymmetric distribution of seasonal biomass, with a short period of chl *a* accumulation in the spring from October to November, high summer production from December to February, the height of the growth season, a fall period from March to the end of May, and a winter that is effectively 4 mo long, from June to September. This pattern is clearest in 2002 (Fig. 8).

The difference in the rate of decrease in biomass in 2002 and 2001 in Palmer Basin indicates that other factors in addition to daylength are of importance. In 2001, although the initial chl *a* in fall was lower than in 2002, chl *a* remained higher through May, but winter biomass minimum was reached a month sooner in 2002 (Fig. 3A). These results suggest that the seasonal pattern and interannual variability in the dynamics of bloom demise creates a variable food

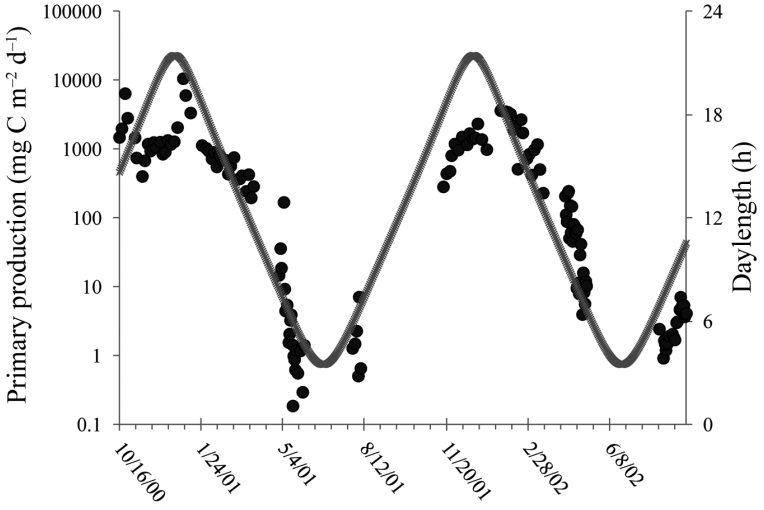

Fig. 8. Seasonal distribution of primary production in the western Antarctic Peninsula from October 2000 to September 2002. Data from the SO GLOBEC fall and winter cruises in 2001 and 2002 and from the Pal LTER seasonal sampling in October to April in 2000 to 2001 and 2001 to 2002 from Palmer Basin (64° S; see 'Materials and methods' for details). Daylength (calculated from Forsythe et al. 1995) is shown by the grey symbols. Dates on *x*-axis are shown as m/d/yy

environment for grazers (including larval krill) during fall, a critical period for zooplankton entering the winter with low phytoplankton availability.

One of the main differences between Palmer Basin and Marguerite Bay is the ~4 wk of winter darkness observed in the south. PP was always positive in Palmer Basin during winter, but reached 0 in Marguerite Bay (Table 3). However, biomass remained rather constant, albeit low, from June to September (Fig. 3). Why does chl *a* not decrease even further and why do concentrations remain constant? Our results highlight the fact that other factors (not considered in the model) are important to explain winter chl *a* concentrations. Periods of sea ice melting, releasing SIMCO to the water column (Ackley et al. 1990), or ridging of sea ice and wave action that can mechanically release particles from sea ice, could maintain winter biomass. In addition, grazing could be limited by the low phytoplankton biomass.

Modeling primary production

In this study, phytoplankton decline during fall was successfully modeled with the bio-optical model of Dierssen et al. (2000) developed for this area. This model has been tested to estimate summer PP in the wAP. As most of the data available for the region concentrate on summer dynamics, the data needed to parameterize the model for fall and winter were scarce. We used Pal LTER fall and SO GLOBEC fall and winter cruises from 2001 and 2002 to extend the summer model. The model is simple but has proven to be robust, with a normalized RMSE of 17.7% for 2001 and 7.7% for 2002. The use of the model allowed us to increase numbers of estimates of PP from weekly measurements to daily estimates, to estimate PP during fall and winter periods when measurements were not available, and to calculate a first approximation of the magnitude of the LFs affecting phytoplankton abundance in the fall that balance growth by photosynthesis.

Chl *a* in wAP coastal waters, in the presence of a mixed layer, is high and uniform within the mixed layer with maximum biomass usually at the surface (Dierssen et al. 2000), similar to models of PP worldwide (Behrenfeld & Falkowski 1997). In this study, modeled PP was calculated as an integrated number within the Z_{eu} and followed the standard curve of maximum PP close to the surface. We have evaluated several areas of parameterization for their impact on this model. First, there is a difference between Z_{eu} and MLD, although this difference decreases as the season progresses and MLD deepens. Chl *a* used as input is the average concentration in the MLD, traditionally not shallower than the depth of 10% PAR (Kozlowski 2008). However, the absence of the production between 10 and 1% light penetration (PAR) could lead to an underestimate of modeled PP. This underestimate would account for only 4 to 6% of the daily PP (calculated from Fig. 3B in Dierssen et al. 2000).

The parameterization of variables in estimating PP (Eq. 2) is critical. *F*, the efficiency of photosynthesis or chl *a*-normalized productivity, has been found to be constant for the season, both in summer (Dierssen et al. 2000) as well as in fall (present study). It is reasonable to suspect that *F* will be lower in winter. In the absence of data, a change in the C:chl *a* ratio could partially account for the expected decrease in efficiency. At high irradiance, $F \approx 1$ and PP(z) will approach P^B_{opt}, albeit modulated by daylength. Fig. 5 shows the shape of PP profiles during early fall (Fig. 5A) and late fall (Fig. 5B), with a decrease in P^B_{opt} due to adaptation to decreasing irradiance as the season progresses. P^B_{opt} is not the maximum short-term surface photosynthetic rate, i.e. not the

value obtained by P (photosynthesis) versus E (irradiance) curves in 1 h incubations (Platt et al. 1980), but is instead an average 24 h P^B_{opt} for the Z_{eu} (see 'Materials and methods'). For example, P versus E curves and 1 h incubations estimate P_{max} in the summer to be as high as 3.5 to 5.1 mg C (mg chl a)$^{-1}$ h^{-1}. In contrast, plotting P versus E curves from the water column with 24 h incubations shows a maximum of 1.2 to 1.5 mg C (mg chl a)$^{-1}$ d^{-1} (Fig. 5). Thus, under conditions of high irradiance, modeled PP approaches the average maximum water column production. P versus E parameters from short-term incubations cannot replace the 24 h experiments, as P_{max} (Platt et al. 1980) would overestimate P^B_{opt}.

The biomass decline in fall and the maintenance of low biomass in the winter results from the calculated LF. Although relatively small, these LFs were important in modeling bloom decline and interannual variability, as shown for 2001 and 2002 in Palmer Basin (Table 3). Without this factor, PP accumulates biomass at a rate dependent on daylength (Fig. 2) and MLD (Table 2), until light disappears. Biomass would not be diluted until MLD > Z_{eu} in mid-June (approximate data, variability is due to water transparency).

Initial fall PP rates were half to one-fourth of summer values (Garibotti et al. 2003, Pearce et al. 2010; our Fig. 8), and decreased even further by June. Estimated growth rates were low (Table 3) as expected during a period of decreasing biomass. Loss rates were similar to growth early in the fall, remaining constant throughout the season (Table 3). By June, loss rates averaged 5 to 10 times higher than growth. At an LF of 6% (as in Marguerite Bay in 2002), growth rates controls biomass accumulation in early fall (μ_i > LR) and ~6% of the PP is 'consumed' or lost daily. As the season progresses and μ_i decreases, the situation reverses, LR > μ_i, and losses outweigh PP for a net biomass decrease. In the absence of sea ice formation, 100% of the daily PP can be consumed by mid-April, and the remaining biomass rapidly disappears thereafter. At an LF of 15% (as in Marguerite Bay in 2001), losses outweigh PP for a net biomass decrease, and growth is always lower than losses (LR > μ_i). By late April, 100% of the daily PP is consumed.

As shown, chl a demise was sensitive to the balance of the parameters determining productivity, mainly P^B_{opt}, F (photosynthetic efficiency), and the C:chl a ratio in addition to losses. However, the higher than expected effect of LF indicates the importance of better identification and parameterization of what affects chl a biomass in the water column. Furthermore, the lack of production data in winter (JJA), generally due to logistical constraints, restricts the ability of the model to provide accurate early spring conditions at the beginning of September. Interestingly, model parameters did document the variability of the fall demise, showing that initial (i.e. 1 March) concentrations were not good indicators of fall biomass.

Environmental factors reducing primary production: scavenging during sea ice formation

The question is: how reasonable are these LFs given our understanding of the ecosystem? The phytoplankton losses as estimated from the modeling and needed to obtain realistic simulation of chl a decline during fall include grazing by macro- and microzooplankton, cell sedimentation and advection, and presumably cell lysis and carbon excretion. Ammonium uptake is also considered to decrease productivity at the end of summer. To evaluate whether phytoplankton losses estimated with the model were realistic, and to assess whether observed and modeled production and biomass are sufficient to maintain zooplankton biomass, we made preliminary calculations of grazing rates for the main species of macrozooplankton and larval krill. These calculations are based on available data for 2001 and 2002, such as summer data for the area from the Palmer LTER project and fall and winter field data from the SO GLOBEC project. In addition, we compared the loss rates (Table 3) to literature values for sea ice scavenging, microzooplankton grazing, sedimentation, etc.

In coastal waters, chl a concentration in the winter can be reduced by scavenging during sea ice formation. During frazil ice formation, ice crystals concentrate particles in the water column. Assuming an average concentration factor of 5.25, we can expect a loss of 50% of the chl a within a 50 m mixed layer during 1 freezing event forming 10 cm of new ice, considerably decreasing phytoplankton biomass (Fritsen et al. 2008). This chl a loss from the water column can continue throughout the season through freezing events in sea ice in response to variability in air temperature. New sea ice in Marguerite Bay in 2001 and 2002 had chl a concentrations 2.7 to 7.8 times those in the underlying water column (Fritsen et al. 2008), even during winter. June is the month of rapid sea ice formation in the wAP (Stammerjohn & Smith 1996). As observed in 2002 in the Marguerite Bay area (Fritsen et al. 2008), high chl a concentrations in winter sea ice were associated with

early sea ice formation which likely entrained phytoplankton from the water column at high concentrations in April and May 2002 (Fig. 3). Enhanced chl *a* concentrations in sea ice provide the basis for SIMCO production. The interaction of timing of fall chl *a* decline with timing of the advance of sea ice and possible SIMCO production may be critical for growth and survival of obligatory grazers, such as larval Antarctic krill, in the winter (Lowe et al. 2012).

Nitrate uptake during fall in productive waters of Antarctica can be inhibited by large concentrations of ammonium, on the order of 8% of the inorganic nitrogen pool (Goeyens et al. 1998). At this time, the *f*-ratio (i.e. nitrate to ammonium uptake) decreases to one-third that of springtime, indicating preference of ammonium uptake over nitrate ($f < 0.5$; Dugdale & Goering 1967, Goeyens et al. 1995). Furthermore, inorganic nitrogen speciation has been shown to be of importance during bloom development (Bode et al. 2002). For our area of study, average ammonium concentrations in the mixed layer in March/April at Palmer Basin (1.92 to 1.19 µM ammonium, 16.41 to 19.04 µM nitrate) were 11.6 and 6.19% of inorganic nitrogen sources in 2001 and 2002, respectively, with significant difference between years (Kruskal-Wallis, $p < 0.01$). In Marguerite Bay, average ammonium concentrations in the mixed layer in early February were also high (1.036 to 1.2 µM ammonium, 13.81 to 17.51 µM nitrate), 6.77 and 7.38% of inorganic nitrogen sources in 2001 and 2002, respectively, with no significant difference between years (Kruskal-Wallis, $p < 0.01$). Later in fall, 2002 ammonium concentrations were lower than in 2001 (Serebrennikova & Fanning 2004). The presence of ammonium reduces chl *a*-specific nitrogen uptake rates and could control productivity at the ice edge toward the end of the growth season (Goeyens et al. 1998) while coastal waters are more heterogeneous (Bode et al. 2002). The decrease in productivity based on ammonium is hypothesized to be as important as grazing pressure in late summer. However, high ammonium concentrations (>10 µM) are found near penguin rookeries at Arthur Harbor during January, at the height of the seasonal growth period (Fig. 8) when chl *a* values can exceed 20 mg m^{-3} (Holm-Hansen et al. 1994, R. C. Smith et al. 2008) and average PP is approximately 1200 mg C m^{-2} d^{-1} (Vernet et al. 2008). In the Bransfield Strait, ammonium contributed 60% of the nitrogen source under bloom conditions (Bode et al. 2002). In Marguerite Bay, co-location of ammonium concentration maxima with areas of highest total inorganic nitrogen and silica deficits was interpreted as a strong spatial coupling between primary and heterotrophic production in fall of 2001 and 2002 (Serebrennikova & Fanning 2004). Thus, nutrients need to be included in future modeling of fall productivity to better understand the role of the potential effect of ammonium to productivity in the wAP.

Macrozooplankton grazers including adult and larval Antarctic krill *Euphausia superba*, the tunicate *Salpa thompsoni*, and the pteropod *Limacina helicina* could potentially have a large impact on phytoplankton (Ross et al. 2008). Most of the herbivorous copepods have migrated to below 500 m or to mid-water column depth for the winter (e.g. Quetin et al. 1996), and thus are not as likely to be important grazers during the period of phytoplankton decline. Grazing rates of these 3 macrozooplanktonic species will depend on their abundance, their size, and the concentration of phytoplankton (chl *a*) in the water column. The estimates based on parameters in Table 4 were used to establish whether modeled fall chl *a* was adequate to support the expected grazing of the phytoplankton during the fall but are not intended to be exhaustive estimates of macrozooplanktonic grazing intensity. Preliminary estimates for the 2 years show substantial differences both between locations and years. The weighted average length (TL, mm) for krill and salps showed spatial and interannual differences (Table 4). The clearance rate (CR) for an individual krill in 2001 was over an order of magnitude greater than in 2002, due to the size differences in the krill between those years (Ross et al. 1998; our Table 4). The CRs for the salps in the Palmer Basin area were generally larger than those found in the Marguerite Bay region. CRs for the pteropod *L. helicina* have yet to be measured due to the difficulties of maintaining this species in conditions that allow for natural feeding and because of differences due to size variations. However, several studies have measured the ingestion rates for *L. helicina* in the Lazarev Sea with pigment methods, assuming 50% chl *a* degradation, with ingestion rates in summer ranging from 2.1 to 6.0 µg pigment $ind.^{-1}$ d^{-1} (as reviewed by Hunt et al. 2008). For our purposes, given that fall phytoplankton concentrations are usually lower than those in summer, we used a constant 2.25 µg pigment $ind.^{-1}$ d^{-1} throughout the fall of both 2001 and 2002 (Table 4). For no species did we consider the effect of temperature, or the influence of cell size distribution on grazing estimates (e.g. Nejstgaard et al. 1995). However, no significant difference between years in cell size was observed in Marguerite Bay (Kruskal-Wallis test, $p = 0.064$). Based on these CRs, pigment ingestion estimates, chl *a* concentration in the water column and a C:chl *a* ratio of 75 (Table 1), fall grazing

Table 4. Macrozooplankton grazing estimates. Abundance (median of 4 stations nearest the modeled station) and weighted average total length (TL) data from the annual cruise for the Palmer LTER for 2001 and 2002. Clearance rates (CR) for adult *Euphausia superba* (Ross et al. 1998, Quetin & Ross 2003) and *Salpa thompsoni* (Madin & Cetta 1984, Perissinotto & Pakhomov 1998) estimated from relationships between size and CR. For *Limacina helicina*, ingestion per individual was expressed in terms of pigment (µg) per day (Hunt et al. 2008)

Species	2001			2002			2001 and 2002
	Median (no. m^{-2})	Mean TL (mm)	CR (l $ind.^{-1}$ d^{-1})	Median (no. m^{-2})	TL (mm)	CR (l $ind.^{-1}$ d^{-1})	Ingestion (µg pigment ind^{-1} d^{-1})
Palmer Basin							
Euphausia superba	0.313	50.41	37.212	2.479	22.26	2.640	
Salpa thompsoni	1.918	32.50	27.399	0.285	23.13	14.636	
Limacina helicina	0.708			9.485			2.25
Marguerite Bay							
Euphausia superba	0.000	42.39	21.205	31.616	19.74	1.795	
Salpa thompsoni	0.000	10.00	3.120	0.046	13.32	5.295	
Limacina helicina	4.643			7.793			2.25

is estimated at 3.6 and ~0.8 mg C m^{-2} d^{-1} in 2001 in Palmer Basin and Marguerite Bay, respectively, and 2.54 and 4.92 mg C m^{-2} d^{-1} during 2002 at the same locations. These losses corresponded to minima of 2.4, 0.0, 0.98, and 3.87%, respectively, of modeled daily PP.

In winter, macrozooplankton grazing is considered negligible due to a decrease in metabolic rates in Antarctic krill (Kawaguchi et al. 1986, Quetin & Ross 1991, Torres et al. 1994), starvation (Ikeda & Dixon 1982), and ingestion rates at about 5% of those in summer (Quetin & Ross 1991). Population cycles of *Salpa thompsoni* are short, so we expect that abundance estimates from January will not hold through the winter, and probably no later than 30 April. Although *Limacina helicina* also have a strong seasonal cycle (Hunt et al. 2008), they reproduce in summer, and by late fall the population is composed primarily of juveniles.

Possible consumption by larval krill can be estimated from abundance, ingestion rate as a function of temperature, chl *a* concentration, larval wet weight (Quetin et al. 2009, Lowe 2010), and larval abundance (P. Wiebe pers. comm.). Ingestion in Palmer Basin was estimated to be between 2.09 and 6.26% of chl *a* standing stock in the fall of 2001, and between 0.03 and 0.05% in the fall of 2002, with a peak in consumption at the end of March for 2001 and the beginning of May for 2002. In Marguerite Bay, 2001 larval ingestion was between 1.24 and 3.8% with peaks on 2 June and 7 July, while in 2002, ingestion was from 0.02 to 0.11% with a peak in consumption on 27 July.

Grazing by heterotrophic protists is estimated to account for a large portion of phytoplankton losses as flagellates feed on picoplankton autotrophs (<0.2 µm) and larger protists on nanoplanktonic phytoplankton (2–20 µm). In addition to cell lysis and exudation, these losses can account for 71% of daily PP (e.g. Lancelot et al. 1991). Measurements of grazing by microzooplankton support these estimates. In polar coastal waters, grazing by microzooplankton can account for 24 to 34% of PP in the summer (Daniels et al. 2006, Pearce et al. 2008), with higher and more variable impact during fall and winter (Pearce et al. 2008). Thus, we can expect microzooplankton grazing to account for a large proportion of daily PP in the 2001 and 2002 fall and winter in coastal waters of the wAP.

Estimation of seasonal sedimentation in coastal wAP can only be speculative. Off Marguerite Bay, sedimentation showed high seasonality, with higher rates in spring and summer and lower in fall and winter. Sedimentation was observed as sinking fecal pellets, detritus, and intact cells (C. R. Smith et al. 2008). C. R. Smith et al. (2008) showed that in this locality, sedimentation in the fall of 2001 was high (18 mg C m^{-2} d^{-1}) and rich in carbon, accounting for approximately 12% of daily PP modeled in their study (their Table 3). Winter sedimentation was 4 times lower at 5 mg C m^{-2} d^{-1} or 17 times higher than the average winter PP. Although the bulk of sedimenting matter is expected to originate from grazing in the form of fecal pellets, low C:chl *a* ratios (C. R. Smith et al. 2008) and direct estimates of intact phytoplankton sedimentation in other studies (von Bodungen et al. 1986, Froneman et al. 2004) indicate that on occasion, cells can contribute significantly to chl *a* loss from the mixed layer. For example, models in the Bellingshausen Sea, during the spring ice edge bloom, assumed senescence at 5% and exudation/lysis at 8% (Murphy et al. 1998).

In summary, preliminary estimates of the combined effect of scavenging during sea ice formation, macro- and microzooplankton grazing, cell sedimentation, carbon excretion, and cell lysis, could consume up to 70% of the daily PP modeled for 2001 and 2002. High rates of loss are mostly episodic (e.g. von Bodungen 1986). In our study area, grazing by macrozooplankton and krill larvae was estimated to be from 0 to 4% and 0.03 to 6.26% of daily PP, respectively. Other grazing, such as by microzooplankton, could consume up to 34% of PP with a more uncertain contribution from other factors. Sea ice formation can make a large difference, by removing up to 50% of the biomass in the mixed layer (>100% of PP) during one freezing event (Fritsen et al. 2008). Our estimated losses are not higher than those reported in the literature for summer conditions, expressed as % of PP. These losses are relatively low, in agreement with the low average sedimentation rates (4% of annual PP) observed at mid-shelf (Ducklow et al. 2008, C. R. Smith et al. 2008). Thus, the chl *a* loss rates obtained from the model suggest that phytoplankton can sustain existing zooplankton populations through the fall, but likely not in winter.

CONCLUSIONS

The model provides a first approximation of the decrease in phytoplankton biomass by 1 order of magnitude during the fall season west of the Antarctic Peninsula. Interannual variability in chl *a* decline was attributed to higher loss rates during 2002 for Palmer Basin while differences between Palmer Basin and Marguerite Bay also include differences in daylength and timing of sea ice formation. The model for Marguerite Bay showed a fall bloom in March to April 2001, the same year that Palmer Basin showed extended fall chl *a* concentrations. In contrast, the fall of 2002 started with higher biomass at both locations and had a rapid decline through the season. Based on preliminary grazing estimates and literature values, the observed LFs of 6.5 to 15% of daily PP needed to accurately model the fall and winter phytoplankton are realistic, even lower than expected. Most of the fall loss could be accounted for by grazing, with the exception of fall of 2002 in Marguerite Bay where early sea ice formation could considerably accelerate loss of phytoplankton biomass through scavenging. Our results suggest that for zooplankton, and for larval krill in particular, decreasing food availability lasts 3 mo from March to June and contains substantial interannual variability, which could be expected to influence winter survival through varying physiological conditions. Data on zooplankton grazing and other loss to PP should be collected at the same time as PP to provide a more accurate picture of fall and winter dynamics. However, in the absence of ancillary data, modeling with a simple but robust model provided a means of obtaining a first approximation to understand the underlying processes.

Acknowledgements. We thank the collaborators and volunteers of the Palmer LTER and SO GLOBEC programs for data collection and analysis (2000–2002). Thanks to K. Sines for invaluable contributions in the field and data analysis; R. C. Smith, K. Ireson, and M. Montes-Hugo for analysis of optical data; K. Pistone for technical help in manuscript preparation; D. G. Martinson and R. Iannuzzi for discussions on mixed layer depth calculations; C. Glé for thoughtful manuscript reviews; and M. Cape for SeaWiFS chl *a* estimates. We gratefully acknowledge the support of Raytheon Polar Services for logistical support in the field, in particular the Station Manager at Palmer, and to the captains and crew of the ASRV 'Nathaniel B. Palmer.' This project was funded by National Science Foundation (NSF) ANT05-PIIAK awards to M.V. (28728), R.M.R. and L.B.Q. (29087), and C.F. (29666), ANT99-GLOBEC awards to M.V. (10175), R.M.R. and L.B.Q. (09933), and C.F. (10098), and OPP96-32763 to the Palmer LTER project; the NSF support is gratefully acknowledged. This is US GLOBEC Contribution no. 719.

LITERATURE CITED

Ackley SF, Smith SJ, Clarke DB (1982) Observations of pack ice properties during the US-USSR Weddell Polynya Expedition. Antarct J US 2:104–106

Ackley S, Lange M, Wadhams P (1990) Snow cover effects on Antarctic sea ice thickness. In: Ackley SF, Weeks WF (eds) Sea ice properties and processes. CRREL Monogr 90:16–22

Behrenfeld MJ, Falkowski PG (1997) Photosynthetic rates derived from satellite-based chlorophyll concentration. Limnol Oceanogr 42:1–20

Bode A, Castro CG, Doval MD, Varela M (2002) New and regenerated production and ammonium regeneration in the western Bransfield Strait region (Antarctica) during phytoplankton bloom conditions in summer. Deep-Sea Res II 49:787–804

Carrillo CJ, Karl DM (1999) Dissolved inorganic carbon pool dynamics in northern Gerlache Strait, Antarctica. J Geophys Res 104:15873–15884

Daly KL (1990) Overwintering development, growth, and feeding of larval *Euphausia superba* in the Antarctic marginal ice zone. Limnol Oceanogr 35:1564–1576

Daniels RM, Richardson TL, Ducklow HW (2006) Food web structure and biogeochemical processes during oceanic phytoplankton blooms: an inverse model analysis. Deep-Sea Res II 53:532–554

Dierssen HM, Smith RC (2000) Bio-optical properties and remote sensing ocean color algorithms for Antarctic Peninsula Waters. J Geophys Res 105:26301–26312

Dierssen HM, Vernet M, Smith RC (2000) Optimizing models for remotely estimating primary production in Antarctic coastal waters. Antarct Sci 12:20–32

Ducklow HW, Erickson M, Kelly J, Montes-Hugo M and others (2008) Particle export from the upper ocean over the continental shelf of the west Antarctic Peninsula: a long-term record, 1992–2007. Deep-Sea Res II 55:2118–2131

Dugdale RC, Goering JJ (1967) Uptake of new and regenerated forms of nitrogen in primary productivity. Limnol Oceanogr 12:196–206

Figueroa FL (2002) Bio-optical characteristics of Gerlache and Bransfield Strait waters during an Antarctic summer cruise. Deep-Sea Res II 49:675–691

Forsythe WC, Rykiel EJ, Stahl RS, Wu HI, Schoolfield RM (1995) A model comparison for daylength as a function of latitude and day of year. Ecol Model 80:87–95

Frazer TK, Quetin LB, Ross RM (1997) Abundance and distribution of larval krill, *Euphausia superba*, associated with annual sea ice in winter. In: Battaglia B, Valencia J, Walton DWH (eds) Antarctic communities: species, structure and survival. Cambridge University Press, New York, NY, p 107–111

Frazer TK, Quetin LB, Ross RM (2002) Energetic demands of larval krill, *Euphausia superba*, in winter. J Exp Mar Biol Ecol 277:157–171

Fritsen CH, Memmott J, Stewart FJ (2008) Inter-annual sea-ice dynamics and micro-algal biomass in winter pack ice of Marguerite Bay, Antarctica. Deep-Sea Res II 55: 2059–2067

Fritsen CH, Memmott JC, Ross RM, Quetin LB, Vernet M, Wirthlin ED (2010) The timing of sea ice formation and exposure to photosynthetically active radiation along the Western Antarctic Peninsula. Polar Biol 34:683–692

Froneman PW, Pakhomov EA, Balarin MG (2004) Size-fractionated phytoplankton biomass, production and biogenic carbon flux in the eastern Atlantic sector of the Southern Ocean in late austral summer 1997–1998. Deep-Sea Res II 51:2715–2729

Garibotti IA, Vernet M, Kozlowski WA, Ferrario ME (2003) Composition and biomass of phytoplankton assemblages in coastal Antarctic waters: a comparison of chemotaxonomic and microscopic analyses. Mar Ecol Prog Ser 247:27–42

Garrison DL, Ackley SF, Buck KR (1983) A physical mechanism for establishing algal populations in frazil ice. Nature 306:363–365

Garrison DL, Buck KR, Reinarts E (1989) Algae concentrated by frazil ice: evidence from laboratory and field measurements. Antarct Sci 1:313–316

Goeyens L, Treguer P, Baumann MEM, Baeyens W, Dehairs F (1995) The leading role of ammonium in the nitrogen uptake regime of Southern Ocean marginal ice zones. J Mar Syst 6:345–361

Goeyens L, Semeneh M, Baumann MEM, Elskens M, Shopova D, Dehairs F (1998) Phytoplanktonic nutrient utilisation and nutrient signature in the Southern Ocean. J Mar Syst 17:143–157

Hofmann EE, Wiebe PH, Costa DP, Torres JJ (2004) An overview of the Southern Ocean Global Ocean Ecosystems Dynamics program. Deep-Sea Res II 51:1921–1924

Holm-Hansen O, Lorenzen C, Homes R, Strickland J (1965) Fluorometric determination of chlorophyll. J Cons Int Explor Mer 30:3–15

Holm-Hansen O, Amos AF, Silva N, Villafañe VE, Helbling EW (1994) *In situ* evidence for a nutrient limitation of phytoplankton growth in pelagic Antarctic waters. Antarct Sci 6:315–324

Hunt BPV, Pakhomov EA, Hosie GW, Siegel V, Ward P, Bernard K (2008) Pteropods in Southern Ocean ecosystems. Prog Oceanogr 78:193–221

Ikeda T, Dixon P (1982) Body shrinkage as a possible overwintering mechanism of the Antarctic krill, *Euphausia superba* Dana. J Exp Mar Biol Ecol 62:143–151

Jeffrey SW, Humphrey GF (1975) New spectrophotometric equations for determining chlorophylls *a*, *b*, c_1 and c_2 in higher-plants, algae and natural phytoplankton. Biochem Physiol Pflanz 167:191–194

Kawaguchi K, Ishikawa S, Matsuda O (1986) The overwintering strategy of Antarctic krill (*Euphausia superba* Dana) under the coastal fast ice off the Ongul Islands in Lutzow-Holm Bay, Antarctica. Mem Natl Inst Polar Res (Jpn) Spec Issue 44:67–85

Kozlowski WA (2008) Pigment derived phytoplankton composition along the western Antarctic Peninsula. MS thesis, San Diego State University, San Diego

Lancelot C, Billen G, Veth C, Becquevort S, Mathot S (1991) Modelling carbon cycling through phytoplankton and microbes in the Scotia-Weddell Sea area during sea ice retreat. Mar Chem 35:305–324

Lowe AT (2010) Simulating growth and condition factor of larval Antarctic krill in response to environmental variability during fall and winter with an individual-based model. MS thesis, University of California, Santa Barbara

Lowe AT, Ross RM, Quetin LB, Vernet M, Fritsen CH (2012) Simulating larval Antarctic krill growth and condition factor during fall and winter in response to environmental variability. Mar Ecol Prog Ser 452:27–43

Madin LP, Cetta CM (1984) The use of gut fluorescence to estimate grazing by oceanic salps. J Plankton Res 6: 475–492

Marrari M, Daly KL, Hu CM (2008) Spatial and temporal variability of SeaWiFS chlorophyll *a* distributions west of the Antarctic Peninsula: implications for krill production. Deep-Sea Res II 55:377–392

Marschall HP (1988) The overwintering strategy of Antarctic krill under the pack-ice of the Weddell Sea. Polar Biol 9: 129–135

Martinson DG, Iannuzzi RA (1998) Antarctic ocean-ice interaction: implications from ocean bulk property distributions in the Weddell gyre. In: Jeffries MO (ed) Antarctic sea ice: physical processes, interactions, and variability, Book 74. American Geological Union, Washington, DC, p 243–271

Meyer B, Atkinson A, Stübing D, Oettl B, Hagen W, Bathmann UV (2002) Feeding and energy budgets of Antarctic krill *Euphausia superba* at the onset of winter — I. Furcilia III larvae. Limnol Oceanogr 47:943–952

Meyer B, Atkinson A, Blume B, Bathmann UV (2003) Feeding and energy budgets of larval Antarctic krill *Euphausia superba* in summer. Mar Ecol Prog Ser 257: 167–177

Meyer B, Fuentes V, Guerra C, Schmidt K and others (2009) Physiology, growth, and development of larval krill *Euphausia superba* in autumn and winter in the Lazarev Sea, Antarctica. Limnol Oceanogr 54:1595–1614

Mitchell BG, Holm-Hansen O (1991a) Observations and modeling of the Antarctic phytoplankton crop in relation to mixing depth. Deep-Sea Res 38:981–1007

Mitchell BG, Holm-Hansen O (1991b) Bio-optical properties of Antarctic Peninsula waters: differentiation from temperate ocean models. Deep-Sea Res 38:1009–1028

Murphy EJ, Boyd PW, Leakey RJG, Atkinson A and others (1998) Carbon flux in ice-ocean-plankton systems of the Bellingshausen Sea during a period of ice retreat. J Mar Syst 17:207–227

Nejstgaard JC, Bamstedt U, Bagoien E, Solberg PT (1995) Algal constraints on copepod grazing. Growth state, toxi-

city, cell size, and season as regulating factors. ICES J Mar Sci 52:347–357

Ott RL, Longnecker M (2001) An introduction to statistical methods and data analysis. Duxbury Wadsworth Group, Pacific Grove, CA

Pakhomov EA, Atkinson A, Meyer B, Oettl B, Bathmann U (2004) Daily rations and growth of larval krill *Euphausia superba* in the Eastern Bellingshausen Sea during austral autumn. Deep-Sea Res II 51:2185–2198

Pearce I, Davidson AT, Wright S, van den Enden R (2008) Seasonal changes in phytoplankton growth and microzooplankton grazing at an Antarctic coastal site. Aquat Microb Ecol 50:157–167

Pearce I, Davidson AT, Thomson PG, Wright S, van den Enden R (2010) Marine microbial ecology off East Antarctica (30–80°E): rates of bacterial and phytoplankton growth and grazing by heterotrophic protists. Deep-Sea Res II 57:849–862

Perissinotto R, Pakhomov EA (1998) The trophic role of the tunicate *Salpa thompsoni* in the Antarctic marine ecosystem. J Mar Syst 17:361–374

Platt T, Jassby AD (1976) The relationship between photosynthesis and light for natural assemblages of coastal marine phytoplankton. J Phycol 12:421–430

Platt T, Gallegos CL, Harrison WG (1980) Photoinhibition of photosynthesis in natural assemblages of marine phytoplankton. J Mar Res 38:687–701

Quetin LB, Ross RM (1991) Behavioral and physiological characteristics of the Antarctic krill, *Euphausia superba*. Am Zool 31:49–63

Quetin LB, Ross RM (2003) Episodic recruitment in Antarctic krill *Euphausia superba* in the Palmer LTER study region. Mar Ecol Prog Ser 259:185–200

Quetin LB, Ross RM, Frazer TK, Haberman KL (1996) Factors affecting distribution and abundance of zooplankton, with an emphasis on Antarctic krill, *Euphausia superba*. In: Ross RM, Hofmann EE, Quetin LB (eds) Foundations for ecological research west of the Antarctic Peninsula, Book 70. American Geophysical Union, Washington, DC, p 357–371

Quetin LB, Ross RM, Frazer TK, Amsler MO, Wyatt-Evans C, Oakes SA (2003) Growth of larval krill, *Euphausia superba*, in fall and winter west of the Antarctic Peninsula. Mar Biol 143:833–843

Quetin LB, Ross RM, Vernet M, Kozlowski W and others (2009) Grazing by larval Antarctic krill and phytoplankton dynamics during the autumn west of the Antarctic Peninsula. Third GLOBEC Open Science Meeting, Victoria, BC (abstract)

Ross RM, Quetin LB, Haberman KL (1998) Interannual and seasonal variability in short-term grazing impact of *Euphausia superba* in nearshore and offshore waters west of the Antarctic Peninsula. J Mar Syst 17:261–273

Ross RM, Quetin LB, Martinson DG, Iannuzzi RA, Stammerjohn SE, Smith RC (2008) Palmer LTER: patterns of distribution of five dominant zooplankton species in the epipelagic zone west of the Antarctic Peninsula, 1993–2004. Deep-Sea Res II 55:2086–2105

Serebrennikova YM, Fanning KA (2004) Nutrients in the Southern Ocean GLOBEC region: variations, water circulation, and cycling. Deep-Sea Res II 51:1981–2002

Smetacek V, Scharek R, Nothig EM, Kerry KR, Hempel G (1990) Seasonal and regional variation in the pelagial and its relationship to the life history cycle of krill. In: Kerry KR, Hempel G (eds) Antarctic ecosystems: ecological change and conservation. Springer, Berlin, p 103–114

Smith CR, Mincks S, DeMaster DJ (2008) The FOODBANCS project: introduction and sinking fluxes of organic carbon, chlorophyll-*a* and phytodetritus on the western Antarctic Peninsula shelf. Deep-Sea Res II 55:2404–2414

Smith RC, Dierssen HM, Vernet M (1996) Phytoplankton biomass and productivity in the western Antarctic Peninsula region. In: Ross RM, Hofmann EE, Quetin LB (eds) Foundations for ecological research west of the Antarctic Peninsula, Book 70. American Geophysical Union, Washington, DC, p 333–356

Smith RC, Baker KS, Byers ML, Stammerjohn SE (1998) Primary productivity of the Palmer Long Term Ecological Research area and the Southern Ocean. J Mar Syst 17:245–259

Smith RC, Martinson DG, Stammerjohn SE, Iannuzzi RA, Ireson K (2008) Bellingshausen and western Antarctic Peninsula region: pigment biomass and sea-ice spatial/temporal distributions and interannual variability. Deep-Sea Res II 55:1945–1963

Stambler N, Lovengreen C, Tilzer MM (1997) The underwater light field in the Bellingshausen and Amundsen Seas (Antarctica). Hydrobiologia 344:41–56

Stammerjohn SE, Smith RC (1996) Spatial and temporal variability of western Antarctic Peninsula sea ice coverage. In: Ross RM, Hofmann EE, Quetin LB (eds) Foundations for ecological research west of the Antarctic Peninsula, Book 70. American Geophysical Union, Washington, DC, p 81–104

Stretch JJ, Hamner PP, Hamner WM, Michel WC, Cook J, Sullivan CW (1988) Foraging behavior of Antarctic krill *Euphausia superba* on sea ice microalgae. Mar Ecol Prog Ser 44:131–139

Torres JJ, Aarset AV, Donnelly J, Hopkins TL, Lancraft TM, Ainley DG (1994) Metabolism of Antarctic micronektonic Crustacea as a function of depth of occurrence and season. Mar Ecol Prog Ser 113:207–219

Vernet M, Martinson D, Iannuzzi R, Stammerjohn S and others (2008) Primary production within the sea-ice zone west of the Antarctic Peninsula: I—Sea ice, summer mixed layer, and irradiance. Deep-Sea Res II 55: 2068–2085

Vernet M, Sines K, Chakos D, Cefarelli AO, Ekern L (2011) Impacts on phytoplankton dynamics by free-drifting icebergs in the NW Weddell Sea. Deep-Sea Res II 58: 1422–1435

von Bodungen B (1986) Phytoplankton growth and krill grazing during spring in the Bransfield Strait, Antarctica—implications from sediment trap collections. Polar Biol 6:153–160

von Bodungen B, Smetacek VS, Tilzer MM, Zeitzschel B (1986) Primary production and sedimentation during spring in the Antarctic Peninsula region. Deep-Sea Res A 33:177–194

Walsh JJ, Dieterle DA, Lenes J (2001) A numerical analysis of carbon dynamics of the Southern Ocean phytoplankton community: the roles of light and grazing in effecting both sequestration of atmospheric CO_2 and food availability to larval krill. Deep-Sea Res I 48:1–48

Waters KJ, Smith RC (1992) Palmer LTER: a sampling grid for the Palmer LTER program. Antarct J US 27: 236–239

Zar JH (1999) Biostatistical analysis, 4th edn. Prentice Hall, Upper Saddle River, NJ

Editorial responsibility: Hans-Heinrich Janssen, Oldendorf/Luhe, Germany

Submitted: April 4, 2011; Accepted: March 5, 2012
Proofs received from author(s): April 12, 2012